Journal of Visualization, Vol. 4, No. 2 (2001) 185-196

A Visualization of a Vector-field by a Homogenized Nascent-particles Tracking

Shirayama, S.*[1] and Ohta, T.*[2]

*1 Department of Environmental & Ocean Engineering, School of Engineering, The University of Tokyo, 7-3-1, Hongo, Bunkyo-ku, Tokyo 113-8656, Japan.
*2 IBM Japan Ltd., 3-2-12, Roppongi, Minato-ku, Tokyo 106-8711, Japan.

Received 8 November, 2000.
Revised 25 February, 2001.

***Abstract*:** Particle tracking methods have been developed to visualize a vector-field. The methods are efficient to show a large-scale and a small-scale structure in the flow field clearly. However, initial positions of the particles sometimes affect a visualized pattern. In addition, when a particle lies on another one, it becomes difficult to display the particle and to recognize the pattern. In this paper, we consider an enhancement of particle tracking methods against those problems. First, we attempt to reduce the dependence of pattern on the initial position and consider how to display a particle occupies another particle position. Essence of our solution is composed of homogenizing nascent-particles and a certain manipulation in a pixel/voxel space. This solution is similar to that of line integral convolution method (LIC). Secondly, accuracy of the visualization process is discussed. Then, we make clear some pitfalls of LIC. Finally, a new technique to overcome drawbacks of conventional particle tracking methods and LIC is described. Several flow fields in two-dimensions and near surfaces are visualized for demonstration of our proposed method.

***Keywords*:** flow visualization, visualization error, vector field, particle tracking method, line integral convolution, homogeneous nascent position.

1. Introduction

A large quantity of data becomes utilized in various fields, and importance of visualization has been pointed out in order to extract useful information from raw data. To summarize and to mine visualized data for analysis are addressed in a chewing process of visualization, and deeply depend on innovating knowledge in each field. This may be named as visualization interpretation. On the other hand, it is considered that a study of visualization technique in computational fluid dynamics has been stagnant according to the spread of general-purpose software. A focus of new development of visualization technique seems to be narrowed down to parallel visualization, real-time visualization, implementation to various kinds of computational environment and speedup of technique. However, the problem of visualization errors was left unsolved. Although several reports have pointed out visualization errors (Buning, 1988; Shirayama, 1995), methods of improvement have not been proposed except iso-contouring, iso-surfacing and time-integral method in particle tracking. In addition, there are some issues related to executing visualization software. Practically, many attempts are required in order to do effective visualization.

In this paper, we remark the inconveniences of visualizing a vector field, and consider a new technique. The visualization technique for a vector field is classified as follows:

- Vector plots (line segments, arrows and tufts)
- Particle tracking (streamlines, pathlines, streaklines and timelines)

- Topology analysis
- LIC (Line Integral Convolution)

In the case of visualizing a vector field, plotting a vector directly and particle tracking are frequently used. Particle tracking may be the most familiar way of the visualization. It has been considered that particle tracking is an easier way to understand structures of global and local regions. However, since the displayed region of particle tracking except a surface streamline exists in the whole computational region, there is a weak point with a great deal of information. Several techniques of grouping the particles like 'ribbon' and 'mesh' have been proposed in order to remove this weak point (Shirayama, 1989). The grouping strategy has been valid to visualize a longitudinal vortical structure in a flow past a three-dimensional body, but if a triple point exists in the flow field, this strategy fails. Status of grouping techniques deeply depends on a characteristic feature of the flow field to be analyzed, and it can be said that generality is lost. Other issues of particle tracking are the followings:

(I) Initial positions of the particles sometimes affect a visualized pattern.

(II) When a particle occupies another particle position, it becomes difficult to display the particle and to recognize the pattern.

We call the issue (I) initial position dependency or nascent position dependency, and call (II) repetitious displaying.

In visualization using a topological concept, a structure of the vector field is recognized by a critical point and a singular line (Hesselink and Helman, 1987; Perry and Chong, 1987; Hesselink, 1988; Globus et al., 1991; Shirayama, 1992). This is the simplest expression of the vector field. However, there are several unsolved problems. A structure of non-linear critical point alters owing to linearization of a local velocity field (Shirayama, 1995). Moreover, the abstracted expression makes it difficult to understand a real flow direction. In particular, when we change the gaze point on a local part from a viewpoint of a global level or on a global from a local, it becomes difficult to recognize the relation between the global and the local structure. On this account, it has been utilized as a method to analyze the flow after a total image of the flow field was grasped. In addition, since the critical point does not always indicate a region of interest as shown in Fig. 1, this method should be combined with

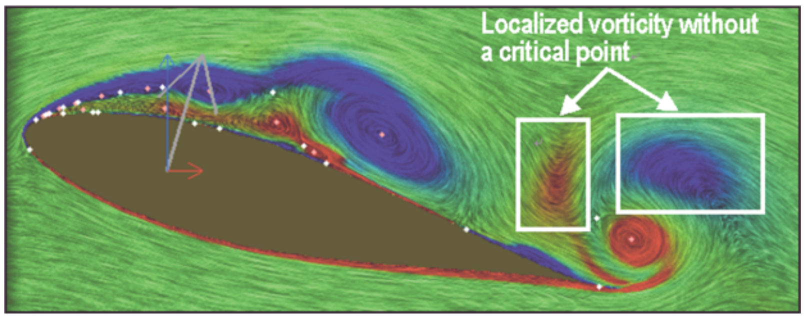

Fig. 1. Vorticity distribution and critical points in a flow around an airfoil.

other techniques.

In visualizing the vector field, the newest method is Line Integral Convolution method (LIC). LIC was originally proposed as a texture mapping in CG (van Wijk, 1991), and has been applied to the flow visualization by Forssell (1994), Stalling and Hege (1995). It may be considered that LIC is a kind of particle tracking methods in an image space. Since particles are basically generated at all pixels, initial positions of the particles do not affect a visualized pattern. In addition, there is no problem of displaying the particles. However, the technique has some pitfalls. Owing to the pitfalls, in visualizing vector data provided from a scientific computation, visualization errors occur. Their images are compared with oil flow patterns, but the reports do not mention visualization errors that give influence to interpretation of visualized results.

In this study, first, several issues in particle tracking method are described. Secondly, we pay an attention to the pixel-based particle tracking in LIC. Then, visualization errors in LIC are pointed out. Finally, a conventional particle tracking method is improved using the ideas of LIC and excluding the pitfalls of LIC.

2. Particle Tracking Method Based on Homogenized Nascent Particles

2.1 Several Issues in Particle Tracking Method

First of all, we summarize issues of conventional particle tracking methods.

The simplest visualization technique for a vector field computed by the Eulerian way is the vector plot. Line segments, arrows or tufts are plotted at the grid points. A pitfall of this approach is that a visualized result depends on the distribution of grid points. Sometimes, some vectors hide a small structure indicated by other vectors, for example, in the boundary layer. If resolution of the grid is higher than that of display, it is said that unnecessary information for the display exists in such region. In the case of large-scale computation, we often encounter this situation.

An example of vector plot for a flow in a channel with abrupt expansion is shown in Fig. 2. It is found that non-uniform beginning positions of vectors and repetitious displaying at the same position by different vectors make it difficult to understand a structure of the flow. In order to prevent these defects, thinning out raw data and sampling interpolated data on a supporting space (ex. equi-spaced rectangular grid system) have been utilized. However, thinning out emphasizes the dependency of patterns on the beginning positions, and sampling causes the alias error. The same issues occur in particle tracking. It is more complicated than the vector plot to thin out raw data since particles move in a grid, from a high to thin density region. Consequently, all the useful information cannot be represented in the region to be visualized. Nascent position dependency cannot be neglected in the case of the visualization of a region near surface, because there are a lot of critical points and singular lines characterize a structure of a three-dimensional flow field.

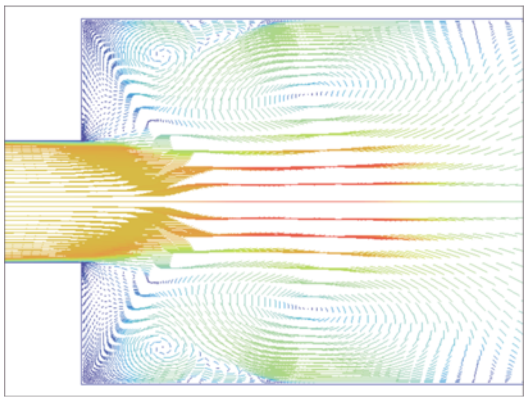

Fig. 2. Vector plots for a velocity field in a channel with abrupt expansion.

Issues in the vector plot and particle tracking are summarized as follows:
(a) it is difficult to balance the resolution of grid and that of display,
(b) repetitious displaying prevents us from getting useful information in the visualized result,
(c) pattern of the visualized result depends on the beginning positions of vector or nascent particle,
(d) all critical points and singular lines cannot be displayed owing to (a) and (b).

2.2 Line Integral Convolution

Line Integral Convolution is a method proposed in Computer Graphics (CG) in order to generate a natural pattern automatically and efficiently. A basic idea of LIC is to determine a color of each pixel using line integral along a vector field in the pixel or the voxel space. It will be expected that methodology of LIC will solve the issues (b) and (c) in the previous section. In order to make the difference between LIC and a proposed method in this paper clear, we explain the procedure of LIC and its pitfalls. For simplicity, a two-dimensional vector field is used.

When LIC is applied to visualizing a computational result, a vector field on the pixel space is extracted as shown in Fig. 3. Then, the procedure of line integral along the vector field from each pixel is performed in the pixel space. If the same way of displaying with the particle tracking method is adopted, a problem of repetitious displaying will occur because a path of integral may exist on another path, but, in LIC, the path is not displayed directly. The color value of each pixel at the starting point of integral is determined by the result of line integral and convolution. This is a significant feature of LIC. We will use it for improving a particle tracking method. From

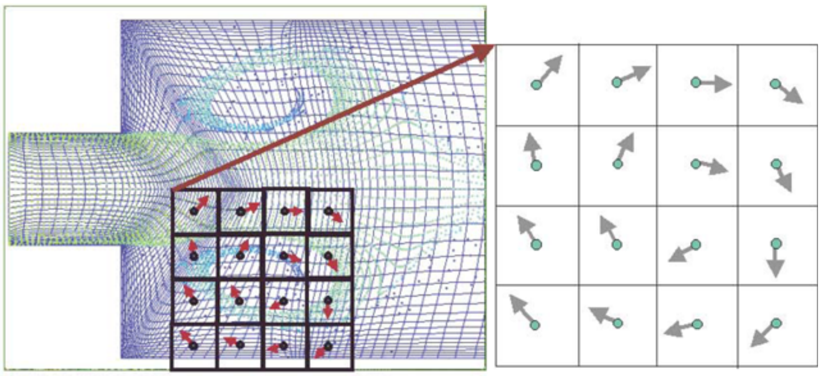

Fig. 3. Sample vectors onto a pixel space.

the different viewpoints, this feature causes pitfalls of LIC. A concrete algorithm of LIC will help us to explain the antithetical nature of LIC.

Let $\boldsymbol{P}$ present a position of a point in the pixel space, and the component is denoted by (i,j). A vector $\boldsymbol{u}$ presents a velocity field in the pixel space. $F(\boldsymbol{P})$ is a certain scalar value on the point; for example, F is brightness. A colored circle in Fig. 4 represents the position of the pixel space and its brightness. Initial brightness of the pixel is mapped from an input image as shown in Fig. 4. Let $\boldsymbol{P}_+^n$ and $\boldsymbol{P}_-^n$ be trajectories along the vector field $\boldsymbol{u}$ starting from $\boldsymbol{P}_0$ in the negative and the positive direction, respectively. The s_+ (positive direction) and the s_- (negative direction) denote a parametric space. The trajectories $\boldsymbol{P}_\pm^n$ are $\boldsymbol{s}_\pm^n$ computed as follows:

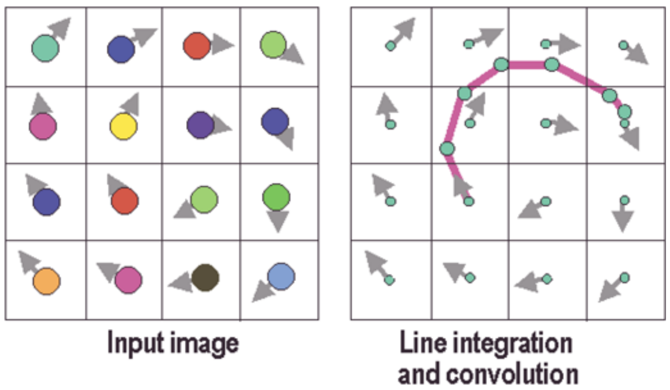

Fig. 4. Input image and integration process in LIC.

$$\boldsymbol{p}_\pm^n = \boldsymbol{p}_\pm^{n-1} \pm \frac{\boldsymbol{u}}{|\boldsymbol{u}|}(Ds_\pm)^{n-1} \tag{1}$$

$$s_\pm^n = s_\pm^{n-1} + (Ds_\pm)^{n-1} \tag{2}$$

where Ds is a certain distance in the parametric space, $\boldsymbol{P}_\pm^0 = \boldsymbol{P}_0$ and $\boldsymbol{s}_\pm^0 = 0$. Let $k(s)$ be a convolution kernel, and we define $h_\pm^n = \int_{s_\pm^n}^{s_\pm^{n+1}} k(w)dw$ (for example, $k(w) = 1$). The resultant brightness F^{new}at $\boldsymbol{P}_0 = (i_0, j_0)$ after LIC process is

$$F^{\text{new}} = \frac{\sum_{n=0}^{N+} F(\boldsymbol{P}_+^n)h_+^n + \sum_{n=0}^{N-} F(\boldsymbol{P}_-^n)h_-^n}{\sum_{n=0}^{N+} h_+^n + \sum_{n=0}^{N-} h_-^n} \tag{3}$$

where $N_\pm$ is total number of steps. The characteristic feature of LIC process is that the brightness of the pixel at the starting point is determined. Therefore, LIC does not have the problem of the repetitious displaying. Figure 5 demonstrates this feature. Usually, a velocity field in a sudden expanded tube drawn at non-uniform grid points produces misleading results owing to the dependence of pattern on the grid location as shown in Fig. 2. In this way, it is found that LIC is one of the powerful tools to visualize a vector field. However, this method has several pitfalls. For the explanation, we will describe the principle of LIC in a rotational vector field (Fig. 6). Eight pixels denoted by A-H are located on a circle as shown in the left side of Fig. 6. When the brightness of the A-H is computed by Eqs.(1) to (3), the values of the brightness at the A-H after the LIC process become almost the same (the right-side of Fig. 6). As a result, the circle appears on the display (the pattern becomes apparent by a convolution of the initial values of the brightness at the pixels being on the integral path).

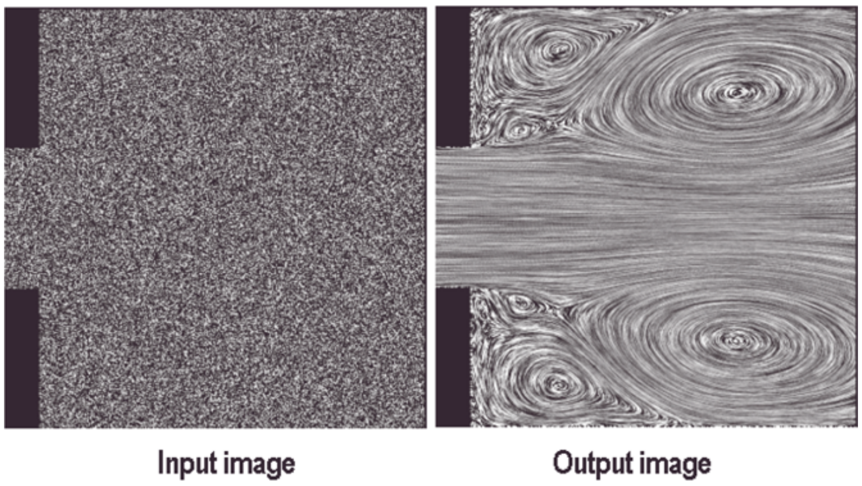

Fig. 5. Visualization of a flow in a channel with abrupt expansion using LIC.

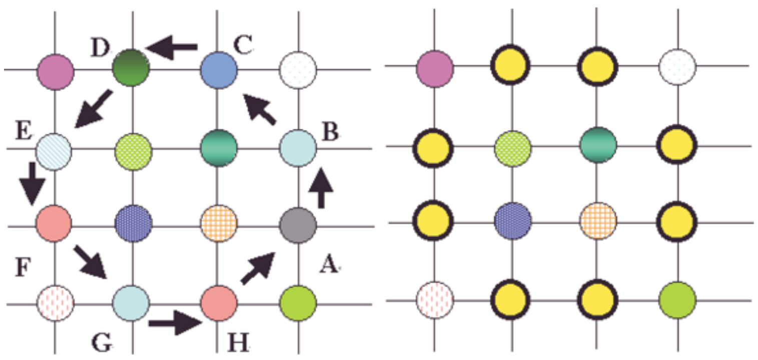

Fig. 6. Mechanism of LIC.

The pitfalls of LIC induced from its procedures are
(i) output image depends on the input image,
(ii) output image depends on the convolution kernel,
(iii) it is difficult to have the consistency of the spatial interpolation in tracking process,
(iv) it is difficult to display the relation between a global and a local structure,
(v) it is difficult to show the magnitude of the vector.
The pitfalls (i) and (ii) have been already pointed out and discussed in CG (see the references (Cabral and Leedom, 1993; Stalling and Hege, 1995) in detail). The issues of (iii) and (iv) are important in visualizing a computed flow field, and are caused by a selection of spatial interpolation method. The difficulty (v) occurs from a principle problem of LIC.

Since the integral and the convolution process are based on the vector field in the pixel space, it may be said that a process of extracting a certain vector on the pixel from raw data is the most important issue. For instance, it becomes the alias error that the resolution of the pixel space eliminates information of the vector field in a high-density grid domain. The errors accumulate in the convolution process, and a difference of the integral path occurs as shown in Fig. 7. Consequently, it can be said that an output image is originally affected by the extraction process.

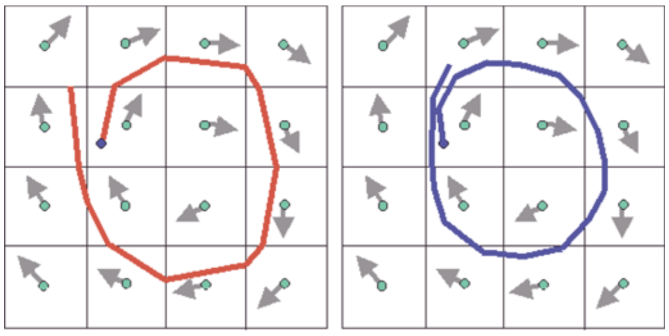

Fig. 7. Errors in LIC.

2.3 Homogenized Nascent-particles Tracking

From the previous considerations, it may be found that the integral and the convolution process have to be improved in order to break off the weak points of LIC. However, this is difficult because the basic principle of LIC should be changed. Therefore, we remark the particle tracking method and alter it using the idea of LIC.

First, we will solve the problem of nascent position dependency. Like starting points of the integration in LIC, homogeneous positions where the particles will be released can be selected using a pixel space. In order to obtain such positions, the computational cell in which each particle lies should be found efficiently. A raster sampling method in a volume rendering (Shirayama, 1991) is applied to obtain the positions. A two-dimensional array N that stands for a pixel space is prepared for the raster sampling. An element of the array is indicated by (i, j). Let (i_{max}, j_{max}) be the maximum size of the array. The index (i, j) also corresponds to a physical location. As shown in Fig. 8, a triangle labeled by k that denotes the computational cell is rasterized, and the label is stored in the array like $N(i, j) = k$. If resolution of the grid is higher than that of the display, we use an over-sampling idea. In most cases, as a huge number of nascent positions are obtained, they are thinned out regularly at need.

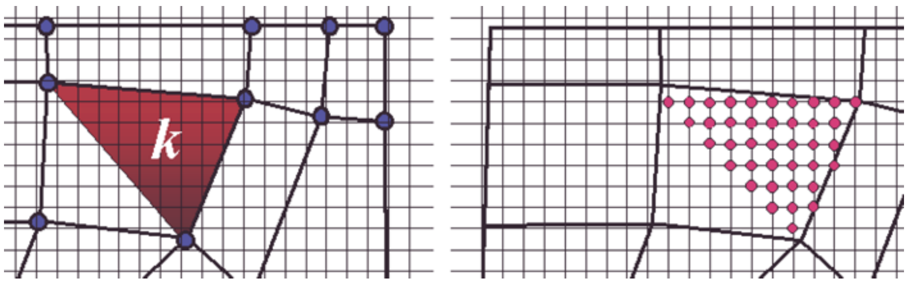

Fig. 8. Raster sampling.

Particle tracking is started from such nascent positions, and the particle proceeds in a physical space as follows:

$$\frac{d\boldsymbol{x}}{ds} = c \tag{4}$$

where $\boldsymbol{x} = \boldsymbol{x}(s)$ is a location of the particle in the physical space and $\boldsymbol{c}$ is a certain vector field. Equation (4) is integrated from the initial location $\boldsymbol{x}^0 = \boldsymbol{x}(0)$ using $\boldsymbol{c}^0$ (the vector at $\boldsymbol{x}^0$). The initial location $\boldsymbol{x}^0$ corresponds to a certain index (i_0, j_0), and is obtained from the computational cell $k_0 = N(i_0, j_0)$. The vector $\boldsymbol{c}^0$ is computed by the same manner. After the initial location is determined using the raster sampling technique, the tracking process is separated from the pixel space. A conventional method will be utilized for the integration of Eq.(4). In this way, we can avoid alias errors in the tracking process.

In the case of raw data from a computational result in the general curvilinear coordinates, we transform Eq. (4) into

$$\frac{d\boldsymbol{X}}{ds} = \boldsymbol{C} \tag{5}$$

where the vector $\boldsymbol{C}$ is the contravariant vector. Let $\boldsymbol{a}^i$ be the contravariant base vector. The component of the vector $\boldsymbol{C}$ (C_i) is calculated by $C_i = \boldsymbol{a}^i \boldsymbol{c}$. Here, $\boldsymbol{\chi}^0$ corresponds to $\boldsymbol{x}^0$ is obtained using the raster sampling.

Secondly, the issue of repetitious displaying will be resolved. The idea of LIC that the final brightness of each pixel is calculated individually will be adopted. We explain it using a concrete algorithm. After homogeneous nascent points are determined, an arbitrary energy field is mapped onto nascent particles. Let the energy be given from an input image, and correspond to a brightness F. Then, particles have the brightness, and flow out along the vector field. The trajectory of the particle is rasterized, and the brightness is distributed to pixels related to the rasterization of the trajectory as shown in Fig. 9. All particles are processed in the same manner, and the output image is composed. The proposed method in this paper is one of the particle tracking methods with the property of LIC. From analogy of the flow visualization technique such that a light reflected by a tracer in a fluid exposes a film, we call our technique Pixel Exposure Method (PEM).

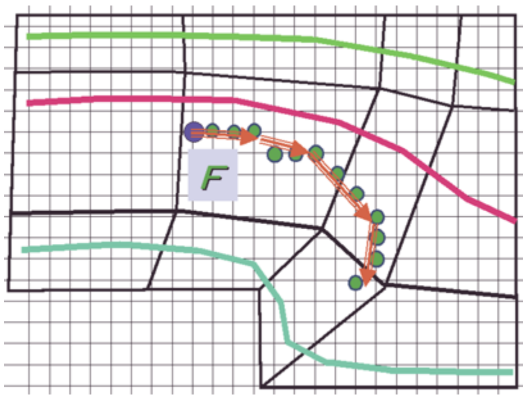

Fig. 9. Computing intensity field using particle tracking and rasterization of line segments.

The pitfalls of LIC mentioned above are revised by PEM as follows.

(i) Dependence of output image on the input image

In general, the dependence of output image on the input image exists in both PEM and LIC. Although a random noise image is often used for a comparison with an experimental result in PEM, we can use a uniform monochrome image for the input. On the other hand, such uniform image cannot be utilized in LIC. It can be said that the dependence is small in PEM.

(ii) Dependence of output image on the convolution kernel

Convolution kernel is not required for PEM.

(iii) Difficulty of having the consistency of the spatial interpolation in tracking process

The Sampling process in LIC does mapping of the vector field itself onto an image space. Furthermore, a line integral corresponds to particle tracking is performed along the sampled vector field. In these two procedures, an alias error occurs and affects the resultant image. On the other hand, the sampling process in PEM is only utilized to determine the positions of the nascent particles, PEM does not have the problem of an alias error. Moreover, tracking the particles is performed in a physical or a computational space, and the alias error does

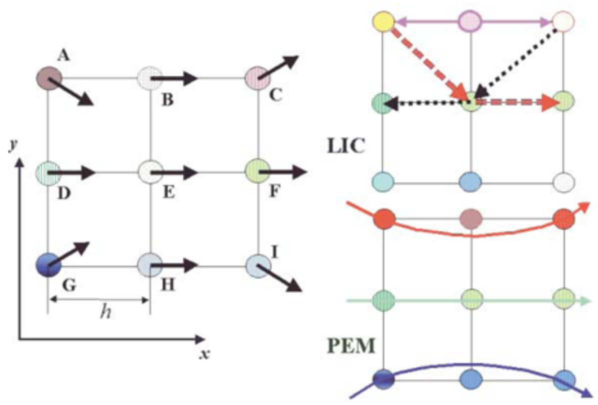

Fig. 10. Difference between LIC and PEM.

not accumulate. For example, we compare LIC and PEM using the following model field: $u = 1, v = \frac{e}{h^3} x^3 \frac{y}{h}$,

where e is an appropriate positive constant and h is the distance between two neighbor pixels (Fig. 10). In Fig. 10, a symbol ○ represents a pixel, and its color shows an input image in the left-hand figure and an output image in the right-hand figure. For simplicity, we assume that upper section (A,B,C) is red series, middle of the stairs (D,E,F) is green series, and the lower berth (G,H,I) consists of blue series. Also, the pixel space and the grid system are in the same location (the origin of the coordinates is shown by E in the figure). In addition, there is no alias error in the sampling process.

Particle tracking of PEM shown in lower part of the right figure is exactly performed according to the model field. Consequently, brightness increases with the same color series in upper, middle and lower parts, respectively. On the other hand, in the case of LIC, for example, the output value of pixel A is computed by A-E-F, and the value of C is done by C-E-D. A color mixes in the upper and lower section. The reason is because the line integration is performed in the pixel space, and the spatial structure of raw data cannot be accounted for the line integration.

(iv) Difficulty of displaying the relation between a global and a local structure

It is difficult to express a global and a local structure in the same figure. A total image of the result is grasped by several figures from different viewpoints. At this point, one important matter is a misleading of a relationship between the global and the local structure. For example, when a vector field as illustrated in Fig. 11 (blue lines in the left-hand figure show the grid system, and a pixel is located at a crossing of a red lattice) is visualized by LIC, a dependency between the pixel A in the global structure and the pixel B in the local structure exists. If a separation line exists between pixel A and pixel B, visualization error occurs. On the other hand, such an error is not produced from PEM because particles are tracked in a physical or computational space.

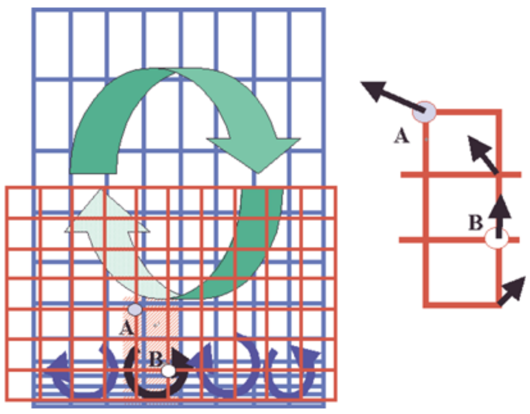

Fig. 11. Visualization error in LIC owing to misunderstanding the local and the global structure.

(v) Difficulty of displaying a magnitude of a vector

In PEM, we can express the magnitude of the vector field without some special treatments, because particles are tracked using the time-increment and the vector field in the flow analysis.

3. Pixel Exposure Method for Arbitrary Surfaces in 3D

In the case that a three-dimensional vector field is visualized by LIC or PEM, a voxel space is utilized. A huge number of operations are required for both methods, and it is too time-consuming to use such visualization techniques. A region to be visualized should be restricted if LIC or PEM can be utilized in practical problems. Therefore, a methodology based on a phenomenon and on a restricted region to be visualized has been proposed (Interrante and Grosch, 1998). This is called ROI (Region Of Interest). The idea of ROI in LIC is interpreted to PEM as follows.

(A) Restrict or thin out the nascent particles according to a phenomenon aimed at investigating.

(B) Restrict a displayed region according to a phenomenon aimed at investigating.

(C) Restrict a domain the particles can move.

In this paper, we extend PEM to visualization of a vector field on a three-dimensional surface. Here, we call PEM in two-dimensions 2D PEM, and do PEM in a three-dimensional surface 3DS PEM. A visualized result by our proposed method will correspond to an oil flow pattern, a pattern of a tuft grid, an image using a laser light sheet etc.

It may be considered that extension from 2D PEM to 3DS PEM can be done directly as the vector field exists in a certain surface defined previously. However, if the raster sampling is uniformly performed on a screen as illustrated in Fig. 12, we cannot obtain homogeneous nascent positions on a body surface. For instance, a point in a certain interval ***d*** on the body surface is mapped on a point in an interval ***s*** on the screen. In the case of LIC on surfaces, some techniques of non-distorted texture mapping have been applied (Forssell, 1994), but it was pointed out by Battke et al. (1997) that such technique is not successful for complex surfaces. In addition, the alias error cannot be avoided in the case that LIC is applied to a scientific computation. Since particle tracking of PEM is performed in a physical or computational space, even if an arrangement of the points where particles are released is a little bit distorted, it may be considered that the output image does not always depend on the sampling process. At first, a computational cell to be rasterized is divided into a triangle element. Secondly, a plane (***Si*** in Fig. 13) which has the same normal vector of the triangle is defined, and resolution of rasterization is determined on this plane. The triangle element is mapped on the plane, and is rasterized in the same manner as 2D PEM. In this way, the nascent positions are determined. Then, the particles are tracked in the physical or the computational space. Finally, the line segments that represent the trajectory of the particle are rasterized on the screen perpendicular to the eye-direction in Fig.12, and the brightness of the particle is added to the pixel in the same manner as 2D PEM. In the rasterization process, hidden-lines are removed.

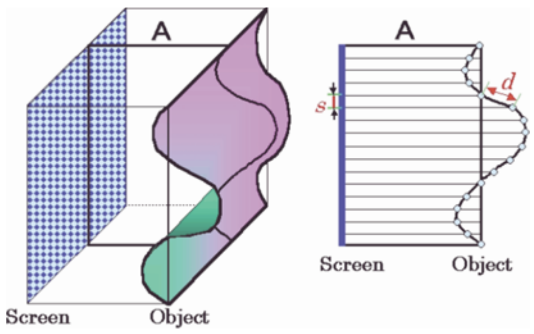

Fig. 12. Sampling error.

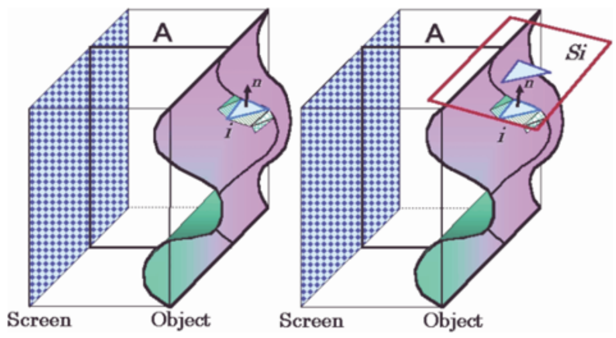

Fig. 13. Raster sampling for arbitrary surface.

4. Results

First, we demonstrate 2D PEM by visualizing a flow in a channel with abrupt expansion (Fig. 14). The procedure of visualization is as follows:

(a) A region to be visualized is defined and temporal nascent positions are determined in the computational space using the raster sampling. In this case, 640×480 positions are obtained.

(b) A uniform random number generates at temporal nascent positions.

(c) Brightness of the particle is proportional to the random number.
(d) The particles whose brightness is more than an appropriate threshold value are released and tracked by Eq.(6).
(e) The brightness of the particle is added to the pixels generated by rasterizing the trajectory as shown in Fig. 9 and the output image is being composed.

Although we thin out the nascent particles by the random number for efficient visualization, it has been found by numerical experiments that to thin out does not mislead the visualized result. Comparing with Fig. 2, there are no initial position dependency and no repetitious displaying in Fig. 14. In addition, the magnitude of the velocity can be expressed. We can show the characteristic region in which a flow converges (where brightness is large).

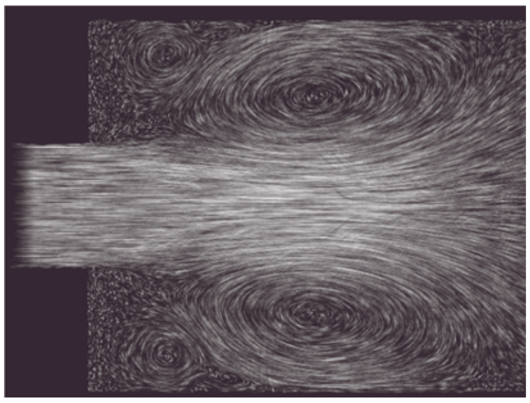

Fig. 14. Pixel exposure method for a flow in a channel with abrupt expansion.

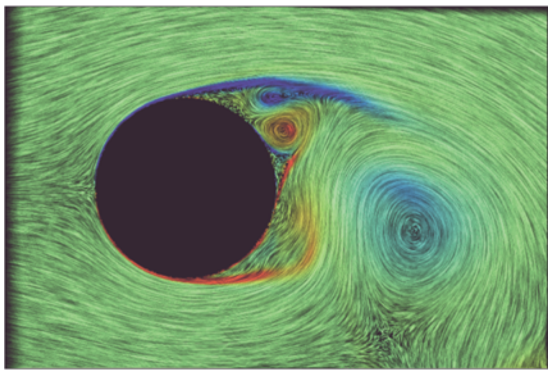

Fig. 15. Pixel exposure method for a flow past a circular cylinder (Re = 10^4, t = 42.5).

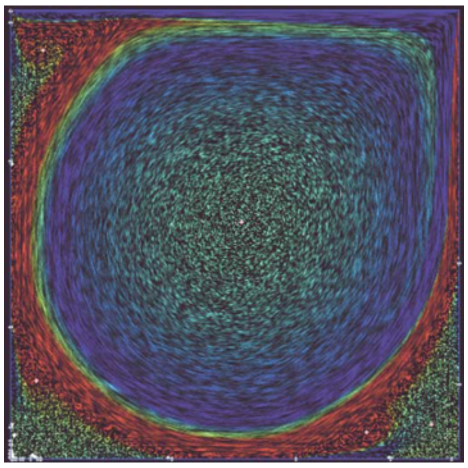

Fig. 16. PEM for a cavity flow (Re = 10^4).

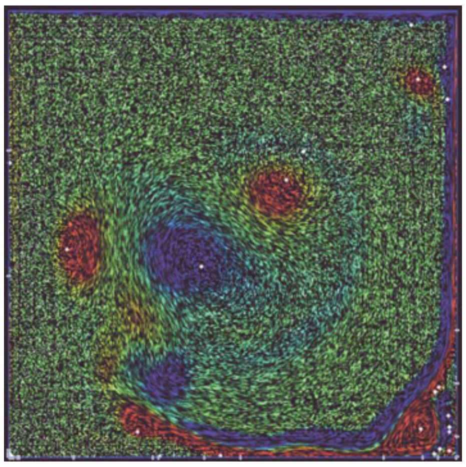

Fig. 17. PEM for a cavity flow (Re = 10^5).

Second examples are visualization of a flow past a circular cylinder and a rid driven cavity flow in two dimensions. Since the output image is composed of the brightness, a certain color map can be overlapped. If a color-shaded pattern of the vorticity is overwritten in the output image, simultaneous expression of the vorticity field and the velocity field can be realized. Figure 15 presents a vorticity and velocity field in a flow past a circular cylinder. A vortex-shedding pattern is clearly visualized by 2D PEM. It was difficult to represent a relation between the localized vorticity and the global velocity field in one figure. Our method can realize it easily. We can demonstrate this advantage in visualization of a rid driven cavity flow with Figs. 16 and 17, definitely. Figure 16 shows a rid driven cavity flow at the Reynolds number 10^4. In this figure, it can be found that the central region of the flow has small vorticity. A rigid rotational flow occupies most of the flow region. The flow at the Reynolds number 10^5 is presented in Fig. 17. It seems that several vortices are generated at the corner and localized near the corner, and then they move into the static flow field. A relation between the vorticity and the velocity is one of the useful information in a mixture of fluid. Our method can show it apparently.

Finally, two examples of 3DS PEM for visualization of a velocity field near a surface are shown in Figs. 18

and 19. Figures 18 and 19 present a flow past a spheroid with angle of attack 15° and a flow past a sphere, respectively. Resolution of rasterization is 500 × 500 for the length of the major axis of the spheroid or the diameter of the sphere. The number of the pixels with no brightness in the region of interest may mean the velocity field that is not visualized. In these figures, there are few pixels with no brightness. That is, all structures like critical points, separation lines and reattached lines on the surface appear in the range of the resolution of the display. However, since the visualization in Figs. 18 and 19 is done by using the direction and the magnitude of the velocity in a region that dynamic range is large such as near the body, it is not always easy to recognize a structure with small velocity. Therefore, we prepare an option that the tangential information is utilized to track the particles. Figure 20 shows such visualization. Structures of the separation lines and reattachment lines appear more clearly than Fig. 19.

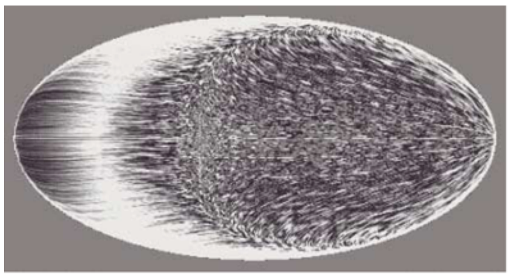

Top view

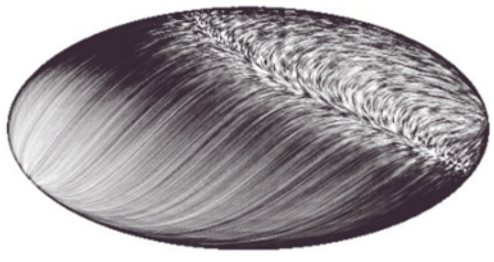

Side view

Fig. 18. Vector field near a surface of a flow past a spheroid.

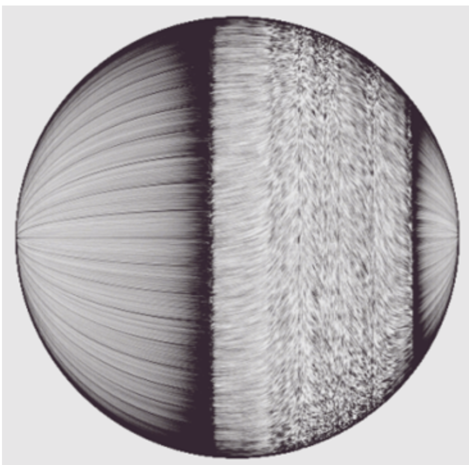

Fig. 19. Flow past a sphere (Re = 10^4).

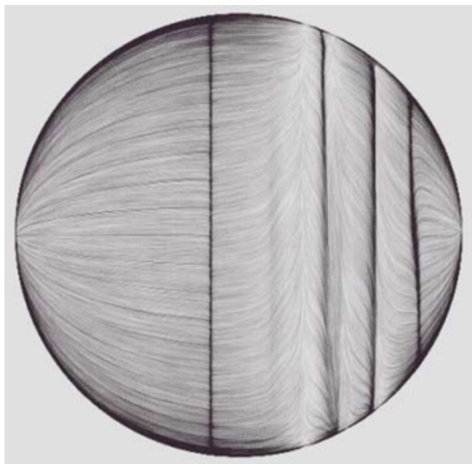

Fig. 20. Vector field is visualized by tangential information near the body surface.

5. Concluding Remarks

We consider a visualization technique to solve the following issues of the vector plot and particle tracking.

(I) Starting points of the vectors and initial positions of the particles sometimes affect a visualized pattern.

(II) When a vector/particle occupies another particle position, it becomes difficult to display the vector/particle and to recognize the pattern.

In the conventional techniques, it is found that LIC is the most appropriate method to solve such issues. However, LIC has other types of pitfalls:

(i) output image depends on the input image,

(ii) output image depends on the convolution kernel,

(iii) it is difficult to have the consistency of the spatial interpolation in tracking process,

(iv) it is difficult to display the relation between a global and a local structure,

(v) it is difficult to show the magnitude of the vector.

We address the issues of the vector plot and particle tracking (I), (II) and the pitfalls of LIC (i)-(v), and propose a new particle tracking method to solve these issues. The method proposed in this paper is as follows. First, homogeneous positions where the particles are released are obtained by a raster sampling. After homogeneous nascent points are determined, an arbitrary energy field is mapped onto nascent particles. Then, particles with the energy flow out along the vector field. The trajectory of the particle is rasterized, and the energy is distributed to pixel. All particles are processed in the same way, and the output image is composed. As tracking the particles is performed in a physical or a computational space the alias error does not accumulate. Moreover, we can express the magnitude of the vector field without some special treatments, because particles are tracked using the time-increment used in the computation. In this way, the issues of the vector plot and particle tracking (I), (II) and the pitfalls of LIC (i)-(v) can be solved. In addition, we extend our method to visualization of a vector field on a 3D surface by contriving a rasterization process. This method will become one of the powerful tools to analyze a vector field obtained from flow analysis.

Acknowledgments

This research is supported by ACT-JST, "Research and Development for Applying Advanced Computational Science and Technology" of Japan Science and Technology Corporation

References

Battke, H., Stalling, D. and Hege, H. C., Fast Line Integral Convolution for Arbitrary Surfaces in 3D, Visualization and Mathematics, (1997),181-195, Springer-Verlag, Heidelberg.

Buning, P. G., Sources of Error in the Graphical Analysis of CFD Results, Journal of Scientific Computing, 3-2 (1988), 149-164.

Cabral, B. and Leedom, L. C., Imaging Vector Fields using Line Integral Convolution, Computer Graphics (SIGGRAPH'93 Proceedings), 27, (1993), 263-272.

Forssell, L. K., Visualizing Flow over Curvilinear Grid Surfaces using Line Integral Convolution, Proceedings of Visualization '94, IEEE, (1994), 240-247.

Globus, A., Levit, C. and Lasinski, T., A Tool for Visualizing the Topology of Three-dimensional Vector Fields, Proceedings of Visualizaton '91, IEEE, (1991), 33-40.

Hesselink, L. and Helman, J. L., Evaluation of Flow Topology from Numerical Data, AIAA-87-1181-CP, Proceedings of the AIAA 8th Computational Fluid Dynamics Conference (Honolulu, Hawaii), (June, 1987).

Hesselink, L., Digital Image Processing in Flow Visualization, Ann. Review of Fluid Mechanics, 20 (1988), 421-485.

Interrante, V. and Grosch, C., Visualizing 3D Flow, IEEE Computer Graphics and Applications, (July/Aug, 1998), 49-53.

Perry, A. E. and Chong, M. S., A Description of Eddying Motions and Flow Patterns using Critical-point Concepts, Ann. Rev. of Fluid Mech., 19 (1987), 125-155

Shirayama, S., A Structure of Leading-edge and Tip Vortices at a Delta Wing, AIAA Paper-89-1803, (June, 1989).

Shirayama, S., Visualization of 3D Unsteady Flow using a Particle Tracing Method, Proceedings of Experimental and Numerical Flow Visualization, FED-128, ASME, (Dec., 1991), 201-208.

Shirayama, S., Flow Past a Sphere: Topological Transitions of the Vorticity Fields, AIAA Journal, 30-2 (1992), 349-358.

Shirayama, S., Processing of Computed Vector Fields for Visualization, Journal of Computational Physics, 106-1 (1993), 30-41.

Shirayama, S., Several Sources of Errors in Numerical Flow Visualization Techniques, AIAA-95-1714-CP, Proceedings of the AIAA 12th Computational Fluid Dynamics Conference (SanDiego, CA), (June, 1995).

Stalling, D. and Hege, H. C., Fast and Resolution Independent Line Integral Convolution, SIGGRAPH95 Conference Proceedings (Los Angeles, CA), (Aug., 1995), 249-256.

van Wijk, J. J. Spot Noise: Texture Synthesis for Data Visualization, Computer Graphics, 25-4 (1991), 309-318.

Author Profile

Susumu Shirayama: He is an associate professor of Environmental and Ocean Engineering at The University of Tokyo. He received his B.Sc.(Eng.) degree in Aeronautical Engineering in 1982 from Kyoto University, and his Ph.D. in Aeronautics in 1987 from The University of Tokyo. His research interest covers scientific and information visualization, large scale data management, high performance computing and computational fluid dynamics.

Takashi Ohta: He is an employee of IBM Japan. He received B.S. and M.S. degrees in Physics from Keio University, in 1985 and 1987, respectively. He received his Ph.D. in Aeronautics in 2000 from The University of Tokyo. He joined IBM in 1990 and has since been working on computer graphics and parallel scientific computation.